Validation of a Customized Method for Estimating Electrical Potentials in the Torso from Atrial Signals: a Computational-Clinical Study

Camila R Restivo[1], Gabriel V Costa[1], Italo Sandoval[1], Maria S Guillem[2], João Salinet[*1]

[1] Federal University of ABC, São Bernardo do Campo, Brazil
[2] Universitat Politècnica de València, València, Spain

Abstract

Atrial fibrillation (AF) is a common supraventricular arrhythmia (SVA) in clinical practice and is characterized by uncoordinated electrical activity of the atria. This study aims to evaluate the influence on the forward solution of AF torso biomarkers under different levels of noise, 3D cardiorespiratory torso/atria morphologies, and number of atria electrodes. 2,048 atrial epicardium electrograms (AEGs) from 5 AF mathematical models were used to estimate 771 body surface potentials (BSPs). The BSPs and respective frequency/phase maps of are obtained after: (i) introduction of noise in the AEGs, (ii) 3D geometry torso/atria modification, and (iii) reduction in electrodes (from 2,048 to 256, 128, 64 e 32; interpolation methods: Linear/Laplacian). To reduce biomarkers disparity, a Butterworth bandpass filter (BPF) at different cut-off frequencies (0.5-30, 3-30 and HDF±1 Hz) is applied on the AEGs prior BSPs estimation. The above methodology is extended to two AF patients (EDGAR database). The estimation of AF BSPs, in different noise ranges, limits the effectiveness of the forward solution. Phase biomarkers are sensitive to the AEGs' pre-processing strategy. The BPF around HDF showed the best agreement between the different SNR levels. Due to the 3D morphological changes, HDF areas variability increased.

1. Introduction

Atrial fibrillation (AF) is the most common cardiac arrhythmia found in clinical practice, affecting about 1% of the world population [1]. Its prevalence increases with age (8% for octogenarians), and it is generally associated with structural cardiac diseases, causing hemodynamic damage and thromboembolic complications with major economic implications [2]. It is estimated that AF accounts for 33% of all arrhythmia admissions [3-5]. This disorder has high morbidity and mortality [6], and it has become a chronic non-infectious cardiovascular epidemic with great consumption of health resources [1,7,8].

Invasive methods provide direct information about atrial activity and has been used to guide catheter ablation therapy of AF. Non-invasive identification of mechanisms using body surface potential mapping (BSPM) can be an important auxiliary tool for clinical outcome planning. In this study, we aimed evaluating the influence on the forward solution AF torso biomarkers under atrial signals noise, morphological torso and atria alteration, and number of atria electrodes.

2. Methodology

2.1. Database

A realistic 3D model of the atrial anatomy composed of 284,578 vertices and 1,353,783 tetrahedra (673.4 ± 130.3 µm between vertices) and of the torso with 771 vertices were used in the analyses. In this work, 5 simulations representing AF originated by driven by functional rotors [9,10] is considered. The simulations have 4 s of duration and the arrhythmia activation frequency ranges between 5.4 and 6.8 Hz. The location of the occurrence of the mechanisms are in RA, RAA, RSPV, LIPV and LPVs. The sampling frequency (fs) of the signals is 500 Hz. In addition, two AF patients are included in the study (data available in the public database EDGAR, http://www.ecg-imaging.org/data-archive). This dataset, for each patient, consists of signals from the torso and atria acquired simultaneously. ECGs were acquired through 54 electrodes and simultaneously, electrograms (EGMs) from the epicardial signals were acquired with a 64-electrode Multipolar Basket Catheters (Constellation, Boston Scientific, Natick, MA) introduced into the left atrium, a standard tetrapolar catheter placed in the coronary sinus, and a 20-electrode catheter placed in the right atrium. The sampling frequency, fs = 2034.5 Hz, is the same for both torso and atria signals.

2.2. Torso electrocardiogram estimation

Body surface potentials are estimated by solving the forward problem with the boundary element method in order to assess the temporal and spatial impact. The 3D geometries of the torso and atria are segmented semi-

automatically through the SEG3D software (https://www.sci.utah.edu/cibc-software/seg3d.html).

2.2.1. Influence of EGM noise effects

White Gaussian noise is added to the atrial signals in different levels (signal-to-noise ratio - SNR: 60, 30, 10, 5, 1 and -3 dB [11]. Then, the signals are pre-processed by a 4th order Butterworth-type bandpass filter, in three different bandwidth strategies: (i) cut-off frequencies between 0.5 Hz and 30 Hz, (ii) 3 Hz and 30 Hz, and (iii) highest dominant frequency (HFD) ± 1 Hz.

2.2.2 Influence on the 3D torso/atria surface modification

The 3D geometries of the aforementioned AF models and the patients were modified according to the respiratory (expiration and inspiration) and cardiac (systole and diastole) cycles. For the torso, 3D geometry is changed as follow: torso is filled in 1/3 of its volume; torso filled with 2/3 of its volume, and full filled, where the geometry referring to the full torso represents the end of inspiration. The changes introduced in the 3D atria morphology are: atrial systole, causing the volume of the ventricles to increase by approximately 25%, early atrial diastole and late atrial diastole, causing elongation of the atria in the direction of the major axis (base to apex) of the heart. Changes were performed through Python 3.

2.2.3. Influence of the number of electrodes

To study the influence of the torso biomarkers due to the different layout of atria electrodes, the number of electrodes from the mathematical models were reduced from 2,048 electrodes to 256, 128, 64 and 32 electrodes [12]. Vertices with unknown potentials are interpolated with Laplacian and Linear interpolation.

2.3. Biomarkers

Eight biomarkers obtained through the frequency maps were calculated: ratio between the mean of the DF and HDF; number of distinct HDF areas; the average size of the HDF(s) in percentage and their average deviation; total area of HDF regions; the interquartile range (IQR) of the DF of all torso vertices; and the average and the IQR of the organization index (OI) in each derivation [13]. From the phase maps, seven biomarkers are calculated: number of filaments per second; average length of filaments in percentage; spatial displacement of the filaments in the torso; number of regions and the size of SP groups; average SP density and bounding box.

2.4. Statistical analysis

Statistical analysis of the distribution was performed using the Kolmogorov-Smirnov statistical method. Variables with positive skewness were normalized using the logarithm to base 10 of the variables. Bilateral analysis of variance (two-way ANOVA) was performed to assess the outcomes of arrhythmia type and morphological changes of the torso and/or atrium, and layout change. In the case of a significant interaction effect, the Post Hoc Bonferroni procedure was performed to identify the source of the difference. Values of $p<0.05$ were considered statistically significant.

3. Results and Discussion

3.1 Influence of EGM noise effects

The 3D maps of DF the torso estimated after filtering the atrial signals around HDF, ensured the most robust approach, preserving the activation frequency estimate, even at high noise levels (-3dB; 78.8% of points of the torso with error < 10%). Furthermore, the pre-processing with the cut-off frequency around the HDF showed the best agreement between the different SNR levels (Figure 1).

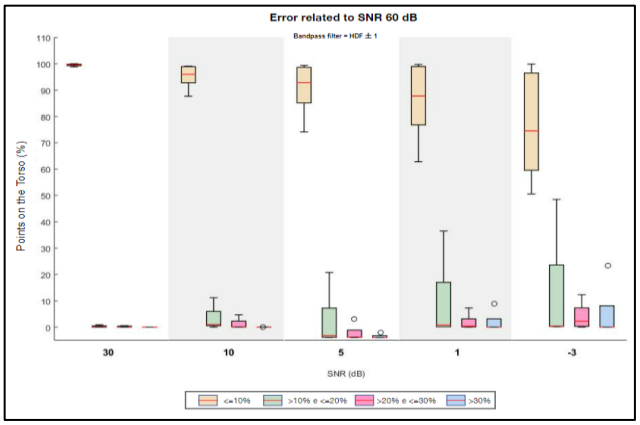

Figure 1: Boxplot of the relative error (boxplot) of the estimated DF related to SNR of 60 dB for the BPF around the highest dominant frequency (HDF ± 1 Hz) in the AF models. HDF: highest dominant frequency.

In general, the phase biomarkers showed to be sensitivity to the pre-processing strategy applied. For example, the filament mean duration (%) obtained at SNR of 5dB spanned between 28.2 ± 1.7 (BPF: 0.5-30 Hz) to 68.1 ± 31.4 (BPF: HDF ± 1 Hz). As in the models, the biomarkers extracted from the phase maps from the AF patients, are also sensitive to the pre-processing strategy applied to the atrial signals, for example: 0,3 filament/s (BPF: 0.5-30 Hz) vs. 0,4 filament/s (BPF: 3-30 Hz) vs. 1.6 filaments/s (BPF: HDF ± 1 Hz).

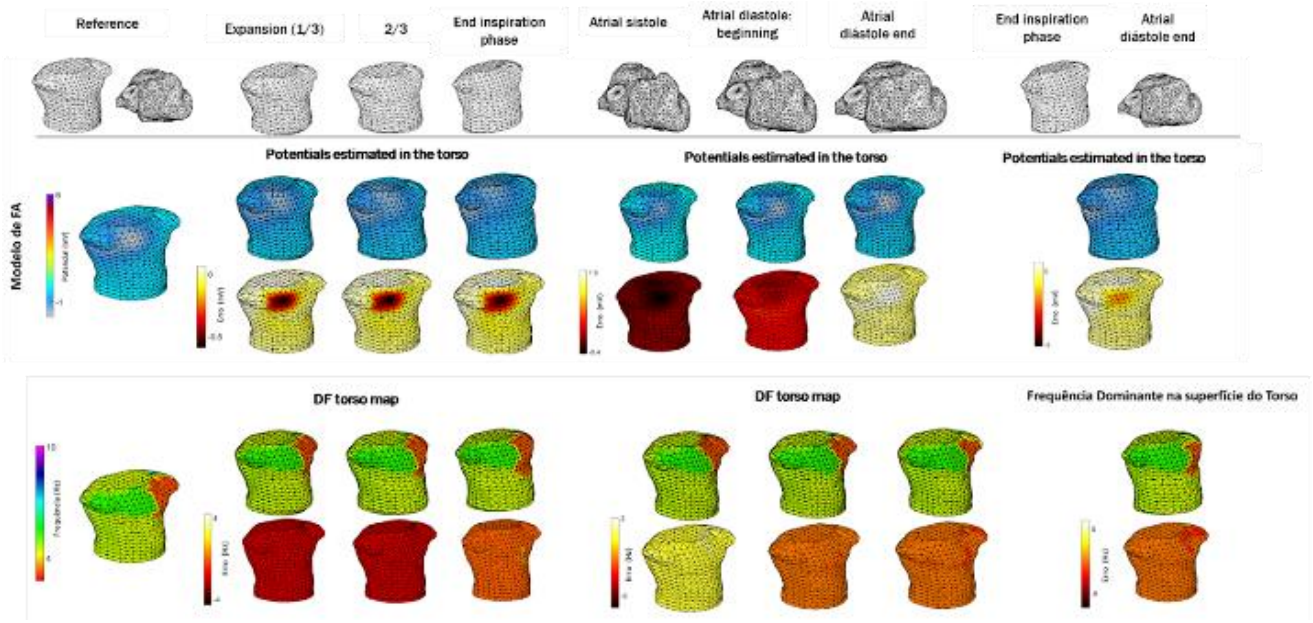

Figure 3: Summary of results over time and frequency for one mathematical model after applying the surface modification. Each pair of lines shows the difference maps and estimates by the forward solution.

3.2 Influence on the 3D torso/atria surface modification

Figure 3 illustrates the impact of the morphological change on the estimation of potentials and frequency of the torso. The first column shows the original geometries, the measured potentials and DF of the torso surface calculated from the measured potentials. The other columns show the change in geometries, the estimated potentials and the DF maps calculated from the potentials estimated by the forward solution and difference maps (relative to the original values).

Due to the morphological changes, although the DF distributions in the AF models did not show significant differences, the mean sizes of the regions (% of the torso) after the morphological changes in the torso underwent changes (Reference; 41.7% ± 47.8% vs. Torso end of inspiration; 36.6% ± 0.2%). In general, there is not a great change in biomarkers according to changes in morphology, but they do change, and therefore it is important that the forward be calculated in the referred phase of the respiratory and cardiac cycle.

3.3 Influence of the interpolation

Figure 4 presents examples of calculated, measured and difference of potentials and frequency for the different numbers of electrodes (i.e. layouts) used. The reduction in the number of electrodes, even with a more robust interpolation method, such as Laplacian, interferes with the potentials calculated by the direct solution, causing considerable errors.

The biomarkers extracted from the phase maps are sensitive to the strategy of reducing the number of electrodes and type of interpolation. This can be observed when analyzing the number of filaments per second with 128 atrial electrodes (771 electrodes: 6.4 ± 1.1 vs Laplacian: 1, 1 ± 0.6 vs simple linear: 2.3 ± 1.5). As expected, according to the reduction in the number of electrodes, the greater the error between the calculated and measured potentials, however there was no linear increase, and the changes vary with the type of arrhythmia. The use of Laplacian interpolation led to smaller errors in the estimation of potentials.

4. Conclusion

The results of the study suggest that the signals in the analyzed cases must be filtered before the estimation of the potentials in the torso, with the bandpass filter around the HDF. Furthermore, when limited number of electrodes is present, it is suggested to apply Laplace interpolation rather linear, prior estimation of torso's signals by the forward solution. Finally, the torso and 3D atria variants morphologies from the cardiorespiratory cycle, should be considered for AF forward solution studies.

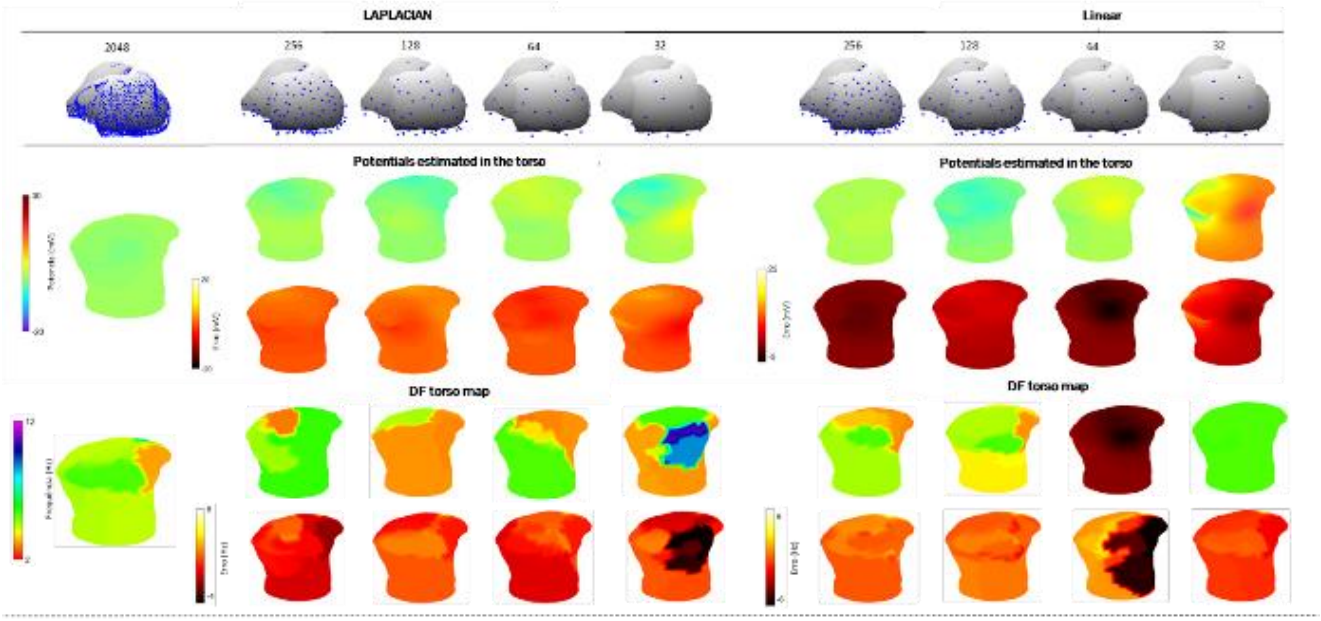

Figure 4: Summary of results over time and frequency for one mathematical model using different types of interpolation. Each pair of lines shows the difference maps and estimates by the forward solution.

Acknowledgments

G.V.C., C.R.R and J.S are supported respectively by grants #2020/13017-2, #2020/12841-3 and #2018/25606-2, São Paulo Research Foundation (FAPESP). M.S.G. received funding from the European Union's Horizon research and Innovation programme under the Marie Skłodowska-Curie grant agreement no. 860974 and the Generalitat Valenciana Grants (ACIF/2020/265). I. Sandoval is supported by Coordenação de Aperfeiçoamento de Pessoal de Nível Superior - Brasil (CAPES).

References

[1] SBC. II Diretrizes brasileiras de fibrilação atrial. Sociedade Brasileira de Cardiologia. Arq Bras Cardiol. 106 (4 supl 2), pp. 1-22, 2016.
[2] Zimerman LI, Fenelon G, Martinelli Filho M, et al. Sociedade Brasileira de Cardiologia. Diretrizes Brasileiras de Fibrilação Atrial. Arq Bras Cardiol, 92 (6 supl. 1), pp. 1–39. 2009.
[3] Bollmann A, Lombardi F. Electrocardiology of atrial fibrillation. Current knowledge and future challenges. IEEE Eng Med Biol Mag, vol. 6, no. 25, pp. 15–23. Nov-Dec. 2006
[4] Lilly LS. Pathophysiology of heart disease: a collaborative project of medical students and faculty. Lippincott Williams & Wilkins. 2012.
[5] Wodchis WP, Bhatia RS, Leblanc K, Meshkat N, Morra D. A review of the cost of atrial fibrillation. Value Health, vol 15, no. 2, pp. 240–8, Mar-Ap. 2012
[6]Naser N, Kulic M, Dilic M, Dzubur A, Durak A, Pepic E, et al. The Cumulative Incidence of Stroke, Myocardial infarction, Heart Failure and Sudden Cardiac Death in Patients with Atrial Fibrillation. Med Arh, vol. 71, no. 5, pp. 316–9, Oct. 2017
[7] Boriani G. The epidemiologic threat of atrial fibrillation: need for secondary, primary, and primordial prevention. Chest, vol. 147 no. 1, pp. 9–10, Jan, 2015.
[8] Staerk L, Sherer JA, Ko D, Benjamin EJ, Helm RH. Atrial Fibrillation: Epidemiology, Pathophysiology, and Clinical Outcomes. Circ Res., vol. 120, no. 9, pp. 1501–17, April. 2017.
[9] Rodrigo M, Climent AM, Liberos A, Fernández-Avilés F, Berenfeld O, Atienza F, et al. Technical considerations on phase mapping for identification of atrial reentrant activity in direct- And inverse-computed electrograms. Circ Arrhythm Electrophysiol, vol. 10, no. 9. 2017 Sep;
[10] Marques VG, Rodrigo M, Guillem MS, Salinet J. Characterization of atrial arrhythmias in body surface potential mapping: A computational study. Comput Biol Med, vol. 127, pp. 103904, Dec. 2020
[11] Oppenheim, A. V.; Discrete-time signal processing. 2. ed. [S.l.]: Pearson, 1996. chap. 10.
[12] Yuksel C. Sample Elimination for Generating Poisson Disk Sample Sets. Comput Graph Forum, vol. 34, no. 2, pp. 25–32, 2015.
[13] Marques VG. Detection of mechanisms. In: Marques, V. G. Characterization of Atrial Fibrillation in Body Surface Potencial Mapping Systems: A Clinical-Computational Study. 2020. Dissertação (Mestrado em Engenharia Biomédica) - Universidade Federal do ABC, [S. l.], 2020.

Address for correspondence:

Camila Rocha Restivo.
Biomedical Engineering, Universidade Federal do ABC (UFABC). Alameda da Universidade s/n, Bairro Anchieta, São Bernardo do Campo, SP, CEP 09606-045, Brazil
camila.restivo@aluno.ufabc.edu.br